Dynamic Proteoids Generated From Dipeptide-Based Monomers

Liu, Yun; Stuart, Marc C A; Buhler, Eric; Hirsch, Anna K H

Published in:
Macromolecular Rapid Communications

DOI:
10.1002/marc.201800099

Publication date:
2018

Macromolecular Rapid Communications
www.mrc-journal.de

Dynamic Proteoids Generated From Dipeptide-Based Monomers

Yun Liu, Marc C. A. Stuart, Eric Buhler, and Anna K. H. Hirsch**

Dynamic proteoids are dynamic covalent analogues of proteins which are generated through the reversible polymerization of amino-acid- or peptide-derived monomers. The authors design and prepare a series of dynamic proteoids based on the reversible polycondensation of six types of dipeptide hydrazides bearing different categories of side chains. The polymerization and structures of biodynamers generated by ^{1}H-NMR spectroscopy, light scattering and cryo-transmission-electron microscopy are studied. This study shows that the presence of aromatic rings in the side chains plays the most essential role in determining the extent of the polymerization and organization into resultant nanostructures through π–π-stacking interactions, hydroxyl groups have a less favorable influence via hydrogen bonds, whereas a high density of positive charge blocks the generation of biodynamers due to electrostatic repulsions. These findings set the stage for the rational design and synthesis of dynamic proteoids as novel biofunctional materials.

1. Introduction

The implementation of dynamic covalent chemistry (DCC)[1–3] in biopolymer science leads to the generation of molecular biodynamers,[4] including DyNAs,[5,6] glycodynamers,[7,8] and dynamic proteoids,[9,10] which are covalent dynamic analogues of nucleic acids, polysaccharides, or proteins, respectively. Due to the inherent nature of reversible covalent bonds and bioactive constituents, molecular biodynamers feature both dynamic character (i.e., changeable, tunable, controllable, self-healing, and stimuli-responsive capacities) and biorelevant properties (i.e., biocompatibility, biodegradability, biofunctionality). As a consequence, they can be employed as adaptive biofunctional biomaterials.[4] Chemists have generated various types of molecular dynamers through the reversible polymerization of nucleobase-, carbohydrate-, amino-acid-, or dipeptide-derived monomers in aqueous media under mild or even physiological conditions to suit their biorelated applications.[10–13] In particular, we reported the design and synthesis of a range of dynamic proteoids based on the polycondensation of different types of amino acid hydrazides with a nonbiological dialdehyde **1** (**Scheme 1**a), through formation of two types of reversible C=N bonds, including both imine and acylhydrazone bonds. As biomimetics of proteins, the construction of dynamic proteoids not only allows understanding protein folding[14] and the relationship between its 3D nanostructure and related biofunction,[15] but may also offer approaches for designing, screening, and generating dynamic inhibitors of protein–protein interactions.[16] The resulting dynamic proteoids possess doubly covalent dynamicity, pH-responsiveness, and potentially a third form of dynamic behavior through structure-formation processes (conformational dynamics). To further improve their biocompatibility, we entirely/partially replaced dialdehyde **1** by a furanose-based dialdehyde to generate a series of saccharide-containing dynamic proteoids by using reversible C=N bond formation with amino acid or dipeptide hydrazides.[13] We found that the property of side chains of amino acid- or dipeptide-based monomers, namely the aromaticity, charge, and polarity, have a strong influence on the rates and extents of polymerization and particle sizes of the resulting dynamic proteoids. The presence of aromatic rings, positive charge, and hydroxyl groups in the side chains can facilitate the polymerization through π–π-stacking interactions, cation–π interactions and hydrogen bonds, respectively. While aromatic rings and positively

Dr. Y. Liu
School of Pharmacy
Guangdong Medical University
Dongguan 523808, China
Dr. Y. Liu, Prof. A. K. H. Hirsch
Stratingh Institute for Chemistry
University of Groningen
Nijenborgh 7, 9747 AG Groningen, The Netherlands
E-mail: Anna.Hirsch@helmholtz-hzi.de
Dr. M. C. A. Stuart
Department of Electron Microscopy
Groningen Biomolecular Sciences and Biotechnology Institute
University of Groningen
Nijenborgh 7, 9747 AG Groningen, The Netherlands
Prof. E. Buhler
Laboratoire Matière et Systèmes Complexes (MSC) UMR 7057
Université Paris Diderot-Paris 7 (Université Sorbonne Paris Cité)
Bâtiment Condorcet, 75205 Paris Cedex 13, France
E-mail: eric.buhler@univ-paris-diderot.fr
Prof. A. K. H. Hirsch
Helmholtz Institute for Pharmaceutical Research Saarland (HIPS) – Helmholtz Centre for Infection Research (HZI)
Department of Drug Design and Optimization (DDOP)
Department of Pharmacy
Campus Building E 8.1
Saarland University
66123 Saarbrücken, Germany
The ORCID identification number(s) for the author(s) of this article can be found under https://doi.org/10.1002/marc.201800099.

DOI: 10.1002/marc.201800099

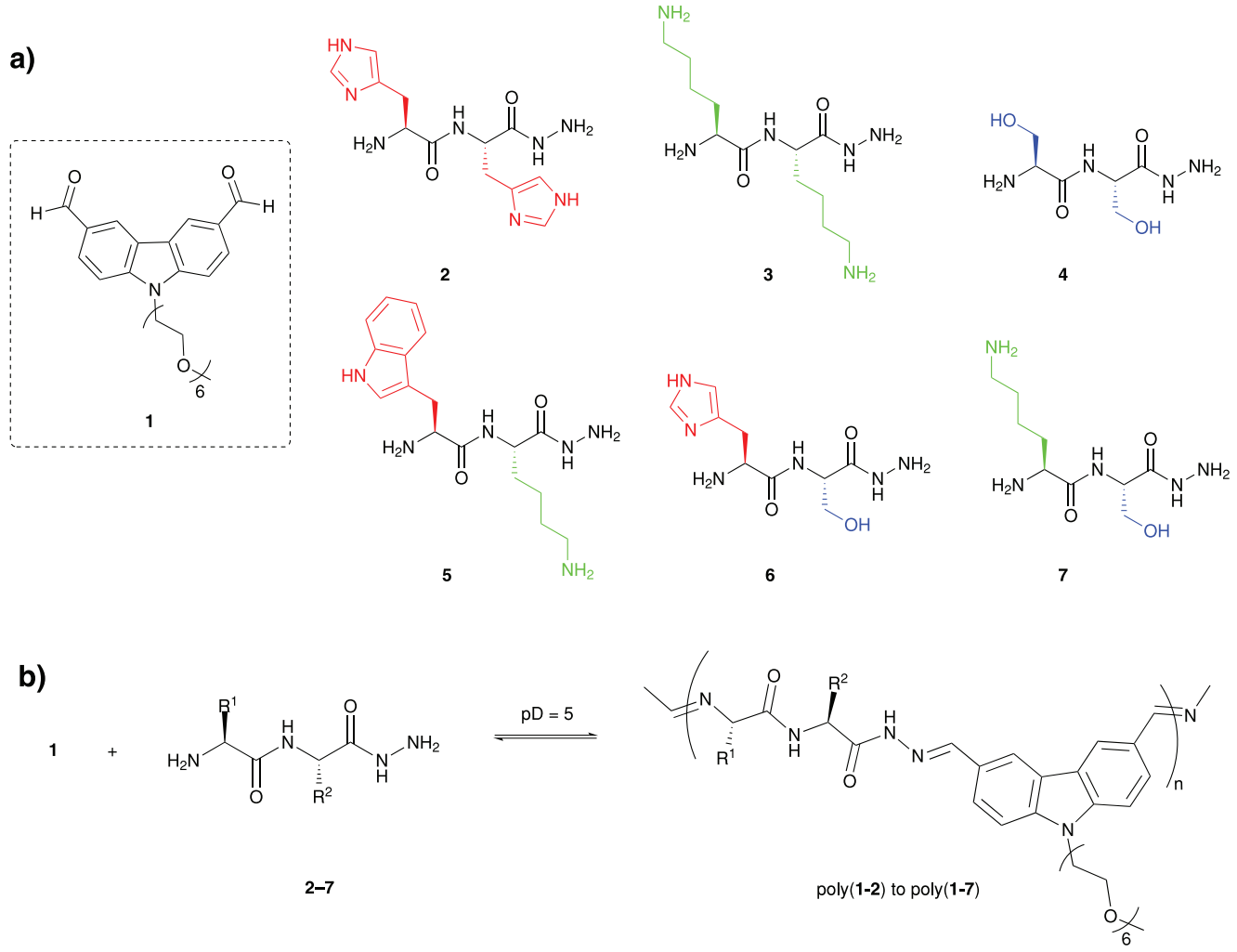

Scheme 1. a) Structures of dialdehyde **1** and dipeptide hydrazides (**2–7**). b) Schematic representation of the preparation of dynamic proteoids through reversible polycondensation of dialdehyde **1** with dipeptide hydrazides **2–7** (aromatic side chains are in red, positively charged side chains in green, and side chains with hydroxyl groups in blue).

charged side chains lead to the generation of dynamic proteoids with globular nano-objects, positively charged side chains give rod-shaped architectures.

However, proteins consist of amino acids with different side chains, which play various roles in protein folding and the formation of their specific 3D nanostructures. Hence, it is necessary to evaluate the varying influence on the rate and extent of polymerization, and particle size of the resulting dynamic proteoids, including aromaticity, positive charge, and polarity of the side chains of the amino acids. Taking into account these considerations, we report here the design and synthesis of a series of dynamic proteoids through reversible polycondensation of aromatic dialdehyde **1** with dipeptide hydrazides **2–7** bearing different side chains (Scheme 1). By studying the polymerization through ^{1}H-NMR spectroscopy and characterizing the biodynamers formed via light scattering (LS) and cryo-transmission-electron microscopy (cyro-TEM), we evaluated the varying importance of the three beneficial factors in determining the rate and extent of polymerization and the organization of the corresponding nanostructures, which benefits the rational design of well-defined nanostructures as adaptive biomaterials.

2. Results and Discussion

2.1. Monomer Design

The enzyme-triggered self-assembly of aromatic peptide amphiphiles into ordered supramolecular nanostructures and their applications in various yields have been extensively studied. Aromatic interactions and hydrogen bonds have been found to play important roles during the formation of nanomaterials.[17,18] In addition, supramolecular hydrogels composed of low-molecular-weight gelators, which can be applied as smart materials, have been prepared through acylhydrazone formation between hydrazides and aldehydes.[19–21] Herein, we prepared dialdehyde **1** and dipeptide hydrazides (**2–7**) as reported previously.[9,13] The aromatic nonbiological dialdehyde **1** consists of a tricyclic carbazole aromatic core and a hexaglyme chain (Scheme 1a).

We have reported that polycondensation of dialdehyde **1** with amino acid hydrazides is driven by hydrophobic interactions derived from the tricyclic core, while the hexaglyme chains endow the resulting biodynamers with water-solubility and stabilize them in aqueous media.[9] Dipeptide hydrazides **2–4** (Scheme 1a) are designed as an enhancement of one beneficial factor, such as two aromatic rings (**2**), two negative charges (**3**), and two hydroxyl groups (**4**). While dipeptide hydrazides **5–7** are a combination of two beneficial factors, including an aromatic ring with a positive charge (**5**), an aromatic ring with a hydroxyl group (**6**), and a positive charge with a hydroxyl group (**7**).[13]

2.2. Generation and Characterization of Biodynamers

The designed biodynamers were synthesized through the polycondensation of dialdehyde **1** with dipeptide hydrazides **2–7** (Scheme 1b). We previously found the mechanism of polymerization to be nucleation–elongation (N–E),[9,22] characterized by the formation of a critical size of polymer chain (nucleus) and elongation of the existing polymer, which is more favorable than initiation of a new chain. Acylhydrazone formation goes to completion at pD 5, whereas the corresponding imine is not formed. However, the reorganization/folding of the resulting dynamic proteoids enabled polymerization, affording the thermodynamic biodynamers as well-ordered nanostructures. We performed the polymerization in aqueous d_3-acetate buffer at pD ≈ 5, conditions where both imines and acylhydrazones are efficiently formed to generate biodynamers. Moreover, we followed the polycondensation by monitoring the signals from the aldehyde group with ^{1}H-NMR spectroscopy (Figure S1, Supporting Information), and calculated the consumption of dialdehyde **1** (Table S1, Supporting Information).

Comparison of the consumption of dialdehyde **1** in formation of poly(**1-2**), poly(**1-3**), and poly(**1-4**) (Table S1, Supporting Information), showed that: 1) aromaticity of the side chain plays the most essential role in facilitating polycondensation, which demonstrates the importance of π–π-stacking interactions. As poly(**1-5**) and poly(**1-6**) contain an aromatic side chain, more dialdehyde **1** was consumed than for poly(**1-3**) and poly(**1-4**); 2) the presence of hydroxyl groups in the side chain has a weaker influence and favors the formation of poly(**1-4**) via hydrogen bonds, which is also confirmed by comparing poly(**1-5**) with poly(**1-6**) in terms of the consumption of dialdehyde **1**; 3) a high density of positive charge (poly(**1-3**)) has a minor effect and blocks polymerization t hrough electrostatic repulsions between side chains; we observed an increment in dialdehyde **1** consumption for poly(**1-5**) and poly(**1-7**) compared to poly(**1-3**). Meanwhile, we investigated the influence of side chains on the rate of polymerization by monitoring the consumption of dialdehyde **1** in equilibrium polymerization (**Figure 1**). Reaction of the dipeptide hydrazides **2–4** and an equimolar amount of dialdehyde 1 afforded the corresponding biodynamer until the ^{1}H-NMR spectra no longer changed after 2 d (consumption of dialdehyde **1**). The generation of poly(**1-2**) is completed in 6 h (Figure 1), which suggests that aromatic rings have the most important influence in accelerating the process of polymerization through π–π-stacking interactions. Poly(**1-4**) reached equilibrium in 1 d, which indicates that hydroxyl groups do not appear to play an important role in accelerating the rate of polymerization. In the formation of positively charged poly(**1-3**), signals from dialdehyde **1** were still visible after 1 week, which illustrates that a high density of positive charge blocks polymerization through electrostatic repulsions. Taken together, these finding are in agreement with the conclusions we drew from monitoring the consumption of dialdehyde **1**.

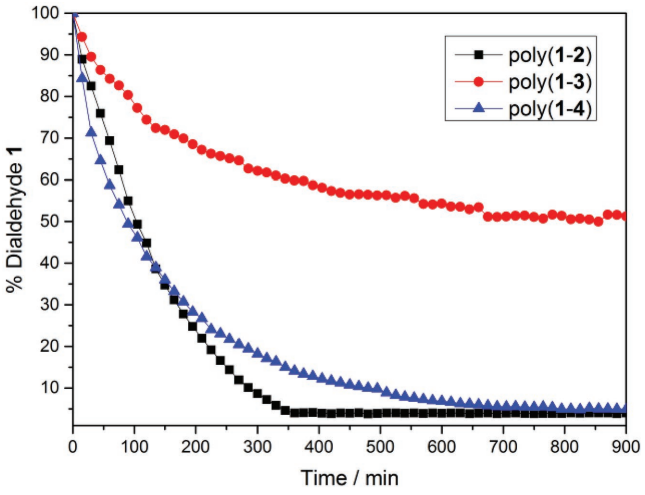

Figure 1. Formation of poly(**1-2**), poly(**1-3**), and poly(**1-4**) in aqueous d_3-acetate buffer at pD 5. Percentage of unreacted dialdehyde **1** versus time.

We investigated the morphologies of resulting biodynamers through dynamic light scattering (DLS), static light scattering (SLS) (**Table 1**; and Figures S2 and S3 and Table S2, Supporting Information) and cryo-TEM (Table 1 and **Figure 2**), given that mass spectrometry does not provide information on the length of the intact biodynamers due to the inherent lability of the imine linkages. The time autocorrelation function of the scattered electric field, $g^{(1)}(q,t)$, obtained from DLS is very well defined and monomodal for all investigated samples and can be described by a simple exponential relaxation showing that solutions are monodisperse and free of large aggregates or impurities (Figure S2, Supporting Information). The angular dependence shows that this relaxation is diffusive with a characteristic time inversely proportioned to q^2, where q is the scattering wave-vector (see the Supporting Information for details), allowing determination of the diffusion coefficient, D, and of the hydrodynamic radius, R_h, of the diffusive particles in dilute solutions (Table 1). Neglecting the excluded volume interactions, the extrapolation to zero-q of the scattered intensity, I ($q^2 = 0$), obtained from SLS provides a direct measure of the apparent weight-average molecular weight of the polymers, $M_{w,app}$, and of the biodynamers aggregation number (see Equations S6 and S7, Supporting Information).

We observed that poly(**1-2**) and poly(**1-6**) have a very large particle size and aggregation number due to the π–π-stacking and hydrogen-bonding interactions, suggesting a different structure than that obtained for the other samples. Poly(**1-2**) and poly(**1-6**) have a $R_h \geq 20$ nm and a radius of gyration, R_g, equal to 48 and 54.3 nm, respectively. Indication on the structure and degree of compactness of the particles is provided here by the $\rho = R_g/R_h$ ratio. The value of this ratio is comprised between 2.4 and 2.66, a value larger than 1, such as for elongated objects or

Table 1. Structural parameters obtained from cryo-TEM and LS.

Sample	R[a)] [nm]	Cross-section radius of nanorods[b)] [nm]	R_h[c)] [nm]	R_h[d)] [nm]	R_g [nm]	M_{dimer} [g mol^{-1}]	$M_{W,app}$ [g mol^{-1}] = KC/I(0)	Aggregation number
Poly(**1-2**)	–	1.55 ± 0.15	20.04	22.10	48	787.9	618 276	785
Poly(**1-3**)	2.52 ± 0.54	–	4.04	5.20	–	770.0	11 739	15
Poly(**1-4**)	–	2.35 ± 0.37	7.94	8.42	–	687.8	252 012	366
Poly(**1-5**)	1.42 ± 0.18	–	2.29	2.64	–	828.0	16 265	20
Poly(**1-6**)	–	1.53 ± 0.15	20.42	20.4	54.3	737.9	579 842	786
Poly(**1-7**)	2.98 ± 0.59	–	4.63	5.39	–	728.9	50 287	69

[a)]Radius of the spherical objects, *R*, obtained from cyro-TEM experiments; [b)]Radius of the cross-section of nanorods obtained from cryo-TEM; [c)]Apparent hydrodynamic radius R_h obtained from DLS measurements by applying the cumulant; [d)]The Contin method to our data. R_g = radius of gyration obtained from SLS measurements for particles larger than 20 nm (i.e., the nanorods). M_{dimer} = dimer molecular weight. $M_{w,app}$ = apparent weight-averaged molecular weight obtained from SLS data extrapolated to zero-*q*. Error bar is ≈5% for R_h and R_g and ≈10% for M_W.

nanorods, which were confirmed by the cryo-TEM observations (Figure 2a,e). In the dilute range, the R_g of rod-like particles with large aspect ratio is given by $R_g^2 = L^2/12$, where L is the contour length of the rod. For poly(**1-2**) and poly(**1-6**) we obtain L = 166 and 188 nm, respectively. It is difficult to determine the average length of these nanorods in cryo-TEM because they adopt many orientations in the 10–300 nm vitrified film. However, the longest structures observed in Figure 2a are parallel to the surface and have a length of the order of that obtained using LS.

The experimental values of the ρ ratio are in good agreement with the theoretically calculated values for cylinders of length L and diameter D given by the following expression in the dilute range: $\rho = R_g/R_h = 1/\sqrt{3}\ \ln(L/D - 0.5)$. Indeed, calculation gives ρ = 2.29 and 2.37 for poly(**1-2**) (L = 166 nm and D = 3.1 nm) and poly(**1-6**) (L = 188 nm and D = 3.06 nm), respectively; i.e., values much larger than one and in good agreement with values obtained from LS. The estimate for the cross-section diameter of the nanorods, D, is provided by the cryo-TEM pictures (Table 1 and Figure 2a,e).

Furthermore, poly(**1-4**) has medium-sized particles and aggregation number owing to hydrogen-bonding interactions, whereas the size of poly(**1-3**), poly(**1-5**), and poly(**1-7**) decreases a lot by virtue of the presence of positive charges. The structure of poly(**1-3**), poly(**1-5**), and poly(**1-7**) is still globular according to cryo-TEM and to the values of the aggregation numbers determined by SLS and of R_h determined by DLS: their sizes are in agreement with the radius $R \approx aN^{1/3}$ calculated for collapsed chains (a being the size of the repeating unit). Although their size is too small for extracting a R_g from the slope of the plot $1/I = f(q^2)$ and then the ρ ratio,

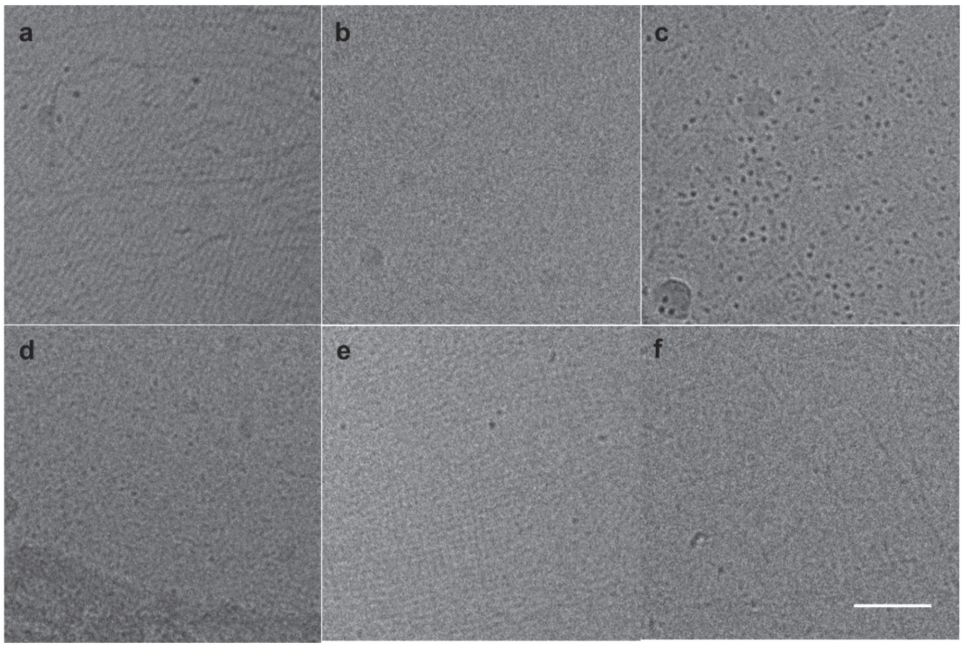

Figure 2. Cryo-TEM images of a) poly(**1-2**); b) poly(**1-3**); c) poly(**1-4**); d) poly(**1-5**); e) poly(**1-6**); f) poly(**1-7**). No stain was used and image acquisition was achieved at a 2 µm defocus. Scale bar = 50 nm.

their shape is most likely that of spheres as confirmed by cryo-TEM showing isotropic objects. These findings are in line with the conclusions from our analysis of the ^{1}H-NMR spectra.

3. Conclusions

In summary, we reported the design and synthesis of a range of dynamic proteoids based on the polycondensation of six dipeptide hydrazides with aromatic dialdehyde **1**, through imine and acylhydrazone formation. By using ^{1}H-NMR spectroscopy, LS, and cryo-TEM, we characterized the polymerization and structures of the biodynamers formed. We evaluated the respective importance of the three beneficial factors and demonstrated that aromaticity of the side chains plays the most essential role in facilitating polycondensation through π–π-stacking interactions, hydroxyl groups in the side chains have a less favorable effect via hydrogen bonds, whereas a high density of positive charge hinders the generation of biodynamers owing to the electrostatic repulsions. Taken together, these findings provide the basis for rational design and synthesis of adaptive dynamic proteoids which behave as novel biofunctional materials and might find their applications in both biomedical and bioengineering fields.

Supporting Information

Supporting Information is available from the Wiley Online Library or from the author.

Acknowledgements

Y.L. was supported by a Ph.D. fellowship from the Chinese Scholarship Council. A.K.H.H. received funding from the Dutch Ministry of Education, Culture and Science (Gravitation Program 024.001.035) and gratefully acknowledges the Netherlands Organisation for Scientific Research (VIDI grant). The authors gratefully acknowledge fruitful discussions with Prof. J.-M. Lehn.

Conflict of Interest

The authors declare no conflict of interest.

Keywords

biodynamers, dynamic proteoids, polycondensation, reversible polymerization, supramolecular structures

Received: February 1, 2018
Revised: March 26, 2018
Published online: May 28, 2018

[1] S. J. Rowan, S. J. Cantrill, G. R. L. Cousins, J. K. M. Sanders, J. F. Stoddart, *Angew. Chem., Int. Ed.* **2002**, *41*, 898.
[2] P. T. Corbett, J. Leclaire, L. Vial, K. R. West, J.-L. Wietor, J. K. M. Sanders, S. Otto, *Chem. Rev.* **2006**, *106*, 3652.
[3] Y. Jin, C. Yu, R. J. Denman, W. Zhang, *Chem. Soc. Rev.* **2013**, *42*, 6634.
[4] Y. Liu, J.-M. Lehn, A. K. H. Hirsch, *Acc. Chem. Res.* **2017**, *50*, 376.
[5] X. Li, Z.-Y. J. Zhan, R. Knipe, D. G. Lynn, *J. Am. Chem. Soc.* **2002**, *124*, 746.
[6] N. Sreenivasachary, D. T. Hickman, D. Sarazin, J.-M. Lehn, *Chem. Eur. J.* **2006**, *12*, 8581.
[7] Y. Ruff, E. Buhler, S.-J. Candau, E. Kesselman, Y. Talmon, J.-M. Lehn, *J. Am. Chem. Soc.* **2010**, *132*, 2573.
[8] P. R. Andreana, W. Xie, H. N. Cheng, L. Qiao, D. J. Murphy, Q.-M. Gu, P. G. Wang, *Org. Lett.* **2002**, *4*, 1863.
[9] A. K. H. Hirsch, E. Buhler, J.-M. Lehn, *J. Am. Chem. Soc.* **2012**, *134*, 4177.
[10] Y. Liu, M. C. A. Stuart, E. Buhler, J.-M. Lehn, A. K. H. Hirsch, *Adv. Funct. Mater.* **2016**, *26*, 6297.
[11] R. E. Kleiner, Y. Brudno, M. E. Birnbaum, D. R. Liu, *J. Am. Chem. Soc.* **2008**, *130*, 4646.
[12] Y. Ruff, J.-M. Lehn, *Angew. Chem., Int. Ed.* **2008**, *47*, 3556.
[13] Y. Liu, M. C. A. Stuart, M. D. Witte, E. Buhler, A. K. H. Hirsch, *Chem. Eur. J.* **2017**, *23*, 16162.
[14] C. M. Dobson, *Nature* **2003**, *426*, 884.
[15] D. Lee, O. Redfern, C. Orengo, *Nat. Rev. Mol. Cell Biol.* **2007**, *8*, 995.
[16] M. R. Arkin, J. A. Wells, *Nat. Rev. Drug Discovery* **2004**, *3*, 301.
[17] J. K. Sahoo, C. G. Pappas, I. R. Sasselli, Y. M. Abul-Haija, R. V. Ulijn, *Angew. Chem.* **2017**, *129*, 6932.
[18] D. Kalafatovic, M. Nobis, J. Son, K. I. Anderson, R. V. Ulijn, *Biomaterials* **2016**, *98*, 192.
[19] F. Trausel, F. Versluis, C. Maity, J. M. Poolman, M. Lovrak, J. H. van Esch, R. Eelkema, *Acc. Chem. Res.* **2016**, *49*, 1440.
[20] S. Mytnyk, A. G. L. Olive, F. Versluis, M. M. Poolman, E. Mendes, R. Eelkema, J. H. van Esch, *Angew. Chem.* **2017**, *56*, 14923.
[21] W. E. M. Noteborn, D. N. H. Zwagerman, V. S. Talens, C. Maity, L. van der Mee, J. M. Poolman, S. Mytnyk, J. H. van Esch, A. Kros, R. Eelkema, R. E. Kieltyka, *Adv. Mater.* **2017**, *29*, 1603769.
[22] D. Zhao, K. Yue, *Macromolecules* **2008**, *41*, 4029.